Remote Sensing of Environment 217 (2018) 191–202

Contents lists available at ScienceDirect

Remote Sensing of Environment

journal homepage: www.elsevier.com/locate/rse

Slowdown of spring green-up advancements in boreal forests

Hoonyoung Park[a], Su-Jong Jeong[b,*], Chang-Hoi Ho[a], Chang-Eui Park[c], Jinwon Kim[d]

[a] School of Earth and Environmental Sciences, Seoul National University, Seoul, Republic of Korea
[b] Graduate School of Environmental Studies, Seoul National University, Seoul, Republic of Korea
[c] School of Environmental Science and Engineering, Southern University of Science and Technology of China (SUSTech), Shenzhen, China
[d] Climate Research Division, National Institute of Meteorological Sciences, Seogwipo, Republic of Korea

ARTICLE INFO

Keywords:
Slowdown of green-up trends
Vegetation phenology
The start of the growing season
Climate change
Boreal forests

ABSTRACT

There is a consensus that the spring phenology of deciduous forests is advancing in response to global warming. Since the late 1990s, however, this tendency of spring phenology advancement has been weakened in over 60% of boreal forests, particularly in Siberia (-0.58 day yr^{-1} for 1982–1997 vs. -0.17 day yr^{-1} for 1982–2013) and northwestern North America (NWNA; -0.42 day yr^{-1} for 1982–1997 vs. 0.07 day yr^{-1} for 1982–2013). This study investigated the major factor in the weakening trends in the advancement of the start of the growing season (SOS) based on the satellite-observed normalized difference vegetation index (NDVI) in two regions by quantifying the effects of four climatic fields—winter duration (WD; the number of freezing days), pre-season temperature (PT; accumulated temperature from late winter to early spring), green-up temperature (GT; accumulated temperature around the green-up date), and pre-season precipitation (PR; accumulated precipitation before the green-up date)—on changes in the spring green-up trend. The GT explained the majority of the slowdown in the SOS trends in recent decades. In Siberia, the GT increases contributed to the advancement of the SOS during the 1980s and 1990s; however, the GT increase reduced to less than half of these periods resulting in a slowdown of the SOS advancing trend since the early 2000s. In NWNA, GT increases and WD shortening drove the SOS advancement until the late 1990s; however, both effects have been diminished to near zero to result in no further SOS advancements. This study demonstrates that the recent slowdown of the SOS advancing trends over Siberia and NWNA was largely attributed to the weakening of the warming trends, rather than the sensitivity changes of spring phenology to climate variables. This study suggests that the natural climate variability strongly affects the decadal variations in the boreal forest spring phenology.

1. Introduction

Vegetation responds to climate most prominently during the growth period (i.e., vegetation growing season) from spring to autumn (Linderholm, 2006). The change in vegetation seasonality is an obvious response of the terrestrial ecosystem to climate and environmental variations as a dynamic component of the Earth system (Bonan, 2008; Pielke et al., 1998). The seasonal cycle of vegetation activity is closely linked to the Earth system and plays a critical role in climate-vegetation interactions (Richardson et al., 2013). From the beginning to the end of the growing season, vegetation interacts with its environment via various processes such as evapotranspiration, carbon uptake, and respiration (Barichivich et al., 2013; Jeong et al., 2009; Peñuelas et al., 2009) with not only regional but also global consequences (Keenan et al., 2014; Myneni et al., 1997; Piao et al., 2007). Thus, changes in the growing season are critical to controlling the interactions among terrestrial ecosystems, climate, and other elements in the Earth system.

Numerous studies have investigated the changes in the growing season using phenology data from spaceborne to ground observations (Garonna et al., 2016; Jeong et al., 2011; Menzel and Fabian, 1999; Piao et al., 2006). Although satellite-based phenology is less reliable than ground observations in studying local ecosystems, it provides a continuous view of terrestrial ecosystems over large areas, and thus is a unique and irreplaceable platform for large-scale vegetation monitoring (Badeck et al., 2004; Delbart et al., 2006; Jeong et al., 2011; Julien and Sobrino, 2009; White et al., 2005). In particular, satellite observations are superior to station data in facilitating the diagnosis of vegetation phenology over vast and inaccessible regions such as boreal forests. With a three-decade time span, satellite-based phenology provides broad knowledge on the mean states and trends in ecosystems, as well as their link with climatic conditions (Myneni et al., 1997; Piao et al., 2007; Jeong et al., 2011; de Jong et al., 2013).

* Corresponding author at: Graduate School of Environmental Studies, Seoul National University, Seoul, Republic of Korea.
E-mail address: waterbell77@gmail.com (S.-J. Jeong).

https://doi.org/10.1016/j.rse.2018.08.012
Received 25 December 2017; Received in revised form 9 August 2018; Accepted 12 August 2018
Available online 20 August 2018
0034-4257/ © 2018 Elsevier Inc. All rights reserved.

In the large-scale vegetation phenology, one of the key topics is the start of the growing season (SOS) which indicates the beginning of biological spring based on satellite imageries (Myneni et al., 1997; Zhang et al., 2003). After the early 1980s, the SOS was becoming earlier worldwide due to global warming (Piao et al., 2007). Although this advancing trend still occurs at a hemispheric scale (Wang et al., 2015), several studies have reported that the strong advancement of SOS during the 1980s and 1990s weakened after the early 2000s over some regions in the Northern Hemisphere (NH), particularly Siberia, northwestern North America (NWNA), the Tibetan Plateau, and Central Europe (Fu et al., 2014a; Jeong et al., 2011; Piao et al., 2011; Wang et al., 2015; Zeng et al., 2011). We call this slowing of the SOS advancement the "green-up slowdown" in the present study.

Detailed mechanisms behind the green-up slowdown remain unclear in NH boreal forests. The slowdown of green-up advancement was reported to be connected to the weakened warming trend after the early 2000s (Fu et al., 2014a; Jeong et al., 2011; Piao et al., 2011; Wang et al., 2015). The majority of previous studies have briefly explained this slowdown of the SOS trend as a result of weakened warming during certain months when the SOS is highly correlated with climate variables (Jeong et al., 2011; Wang et al., 2015). Spring phenology is affected in a complex way by various environmental factors from winter senescence to the green-up season (Hänninen and Kramer, 2007). The process of leaf development is sensitive to temporary warm or cold spells during the green-up period as well as in the preceding period, and the effects of prolonged cold weather in early spring can be compensated for by exceptional warmth during the green-up period (Richardson et al., 2009). Therefore, overall temperature variations from winter to spring should be considered for possible offsetting by temperature conditions during different periods. Precipitation may also play a complementary role during the slowdown of green-up trends (Fu et al., 2014b; Li et al., 2017).

This complexity in spring phenology must be taken into account to comprehend details of climatological processes; however, to the best of our knowledge, no previous study has focused on the effects of multiple climatic variables on the green-up slowdown over vast forests in the NH. Several studies have suggested that the slowdown is related to the warming in winter and spring; however, these are geographically confined to specific regions such as the Tibetan Plateau (Piao et al., 2011; Yu et al., 2010) and western Central Europe (Fu et al., 2014a). These findings in regional studies showed the necessity for examining multiple factors to explain the green-up slowdown. For NH boreal forests, however, the importance of possible factors and their influences on the green-up trend remain unknown.

This study aims to explain the major factors in the recent slowdown of the vegetation green-up date in the NH boreal forests using linear relationships between multiple variables. By focusing on the effects of multiple climate variables, we expect to gain insights into the relative importance of individual variables on the observed SOS trend, as well as the climatic mechanisms of the green-up slowdown during the recent decade.

2. Materials and methods

2.1. Dataset

The SOS over the high-latitude regions of the NH ($> 45^{\circ}$N) was estimated from the third-generation normalized difference vegetation index ($NDVI_{3g}$) produced by the Global Inventory Monitoring and Modeling System (GIMMS) project (Pinzon and Tucker, 2014), which covers the entire Earth surface with a $1/12^{\circ}$ latitude-longitude grid and a 15-day interval from July 1981 to December 2013. Quality of the GIMMS $NDVI_{3g}$ was improved based on multiple-sensor recalibration, especially in high-latitude regions (Pinzon and Tucker, 2014). A bi-weekly maximum composite method and other calibrations were performed to reduce data contamination by other effects such as snow and cloud which are not involved in vegetation changes (Pinzon and Tucker, 2014). The GIMMS $NDVI_{3g}$ dataset is the longest continuous and non-stationary dataset of global vegetation activities, hence is suitable for analyzing trends. Because of this strength, the dataset proved its usefulness for investigating large-scale vegetation activity in a number of previous studies (e.g., Cong et al., 2013; de Jong et al., 2013; Garonna et al., 2016).

A global land cover classification of 1-km pixel resolutions created by the University of Maryland (UMd) was utilized to extract data for boreal deciduous forest regions (Hansen et al., 2000). Among the fourteen land cover classes in the classification, only four deciduous forest types—deciduous needleleaf forests, deciduous broadleaf forests, mixed forests, and woodlands—were analyzed in the present study. A majority resampling approach was applied to the UMd land cover classification for consistency between the finer resolution of the UMd land cover (1 km) and the GIMMS $NDVI_{3g}$ (~8 km) (de Jong et al., 2013; Park et al., 2015). Additionally, the region where the difference between winter mean (January–March) NDVI and summer mean (June–August) NDVI below 0.3 was regarded as evergreen type and excluded from the present analysis.

The SOS was obtained as the date of the inflection point of the NDVI logistic curve at individual grid points in the region of interest for the entire period (1982–2013). A logistic curve was fitted to the NDVI time series from the first positive to the maximum value in a year (see Park et al., 2015 for details). We also excluded negative NDVI values to alleviate possible effects of snow to minimize errors in SOS determination. The logistic-curve fitting has been found to be appropriate for describing the transitional stage from winter dormancy to summer maturity (Julien and Sobrino, 2009; Zhang et al., 2003).

Daily temperature and precipitation measurements were obtained from the ERA-Interim reanalysis dataset (Dee et al., 2011) provided by the European Center for Medium Range Forecasts, one of the most widely applied reanalysis data for various weather and climate research (Bastos et al., 2017; Li et al., 2015). This study utilized the $0.75^{\circ} \times 0.75^{\circ}$ resolution ERA-Interim dataset at one-day intervals so that the spatial resolution (i.e., the area represented by individual data points) of the meteorological data was comparable to that of the NDVI data. The temperature and precipitation data in the ERA-Interim reanalysis were sampled using the nearest-neighbor interpolation scheme to the $NDVI_{3g}$ data points.

For the climate fields that can affect spring phenology, we selected winter duration (WD; the number of freezing days), pre-season temperature (PT; accumulated temperature from late winter to early spring), green-up temperature (GT; accumulated temperature around the green-up date), and pre-season precipitation (PR; accumulated precipitation before the green-up date). These four variables were selected to represent the general characteristics of the environmental conditions that can influence spring phenology on the basis of the traditional growing degree-day (GDD) concept. The GDD, defined as the amount of accumulated temperature from winter to spring above a certain temperature threshold, was established in a number of previous studies on spring phenology for understanding the effects of the changes in spring temperature conditions on spring phenology (e.g., Cannell and Smith, 1983; Cook et al., 2012; Ho et al., 2006; Melaas et al., 2016). We divided the GDD into three sub-components associated with WD, PT, and GT of different temporal windows. This partitioning of accumulated temperature for different time periods was for considering possible offsets among these temperature variables as found in earlier studies (e.g., Richardson et al., 2009). Also, PR was included to consider the effects of precipitation on spring phenology (Fu et al., 2014b; Richardson et al., 2013). We also examined the role of radiation on the SOS advancement trends; however, radiation was strongly correlated with temperatures in boreal forests and thus was excluded to avoid the collinearity problem in multilinear regression.

In addition, we conducted a partial correlation analysis between the SOS and these four variables to examine how closely these climate

fields are related to spring phenology (Peng et al., 2013). Partial correlation measures association between two variables (i.e., independent and explanatory variables) without influences of other variables (i.e., controlling variables). This method is effective to check the relationship between the SOS and multiple climate variables.

The WD, PT, GT, and PR were computed at each SOS pixel and year as follows:

$$\mathrm{WD} = \sum_{t=t_0}^{SOS_{clim}} \begin{cases} 0 \; for \; T(t) \geq T_0 \\ 1 \; for \; T(t) < T_0 \end{cases}, \tag{1}$$

$$\mathrm{PT} = \sum_{t=SOS_{clim}-75}^{SOS_{clim}-16} T(t), \tag{2}$$

$$\mathrm{GT} = \sum_{t=SOS_{clim}-15}^{SOS_{clim}+15} T(t), \tag{3}$$

$$\mathrm{PR} = \sum_{t=SOS_{clim}-59}^{SOS_{clim}} P(t). \tag{4}$$

The ERA-Interim daily temperature and precipitation are denoted by $T(t)$ and $P(t)$, respectively, as a function of the day of a year (i.e., t). The climatological SOS, the SOS_{clim}, is the mean SOS value during the entire period at each data point. The start date of accumulation and the temperature threshold, t_0 and T_0, were set to the first day of the year and 0 °C, respectively. Tests with different start dates (e.g., the winter solstice of the last year) and thresholds (e.g., 5 °C) showed similar results as presented in this study.

First, the WD was defined as the number of days when $T(t)$ was lower than 0 °C. The WD measures the degree of cold exposure that hinders plant metabolism and retards the start of vegetation functions. The WD has a larger value in a year of lingering winter or greater than normal freezing days during early spring. Although chill exposure controls the heat requirement for spring phenology (Cannell and Smith, 1983), its effects were not included in the present study because chilling requirements remain unknown (Melaas et al., 2016). Fig. 1a shows the partial correlation between the SOS and WD without the influences of the other three climate fields. The SOS was positively correlated with WD in high-latitude regions such as Siberia and northern parts of North America. The positive relationship between the SOS and the WD implies that more frequent freezing days (i.e., larger WD conditions) delay the SOS for boreal forests. By contrast, the correlations were relatively weaker in Europe than in other regions along the same latitude, indicating the WD minimally affected the interannual variations in the SOS in Europe.

Second, the PT was defined as the accumulation of temperatures during the pre-season period from 75 days to 16 days, i.e., the heat accumulated for the 2-month period before the climatological SOS (Cong et al., 2013; Wang et al., 2015). This concept of antecedent temperature history is widely applied to the understanding of the relationship between the pre-season temperatures and the SOS changes (Fu et al., 2014a; Jeong et al., 2011; Piao et al., 2011; Wang et al., 2015). In Fig. 1b, the PT shows negative correlations, particularly in Europe and eastern North America, with higher PTs leading to earlier SOSs. In contrast, this relationship was weak or even positive in high-latitude regions such as Siberia and the northern parts of Eurasia and North America. This indicates that the vegetation activity in the Arctic region is not responsive to the PT unlike in other regions.

Third, the GT was defined as the accumulated temperature during the green-up period, 31 days around the climatological SOS. Temperatures during different periods can influence spring phenology differently (e.g., delaying the effect by a cold spell in early spring or advancing the effect by a large warmth during the green-up period); they can even cancel the influences of other fields (Richardson et al., 2009). Thus, we employed two temperature values, PT and GT, with diverse time windows to consider their impacts separately. In Fig. 1c, the GT shows generally negative relationships with the SOS over the entire study region in contrast to the latitudinal dependency in the WD and PT. This negative correlation means earlier green-up is strongly related to higher temperature conditions during the green-up period. The negative relationship between the SOS and the GT occurred over the entire study region and was stronger in northern Eurasia than other regions including North America in the same latitude.

Finally, the PR was defined as accumulated precipitation during the two months preceding the climatological SOS. Precipitation is a relatively minor variable for spring green-up; however, it can play a supportive role in vegetation growth in water-limited regions (Cong et al., 2013). In high-latitude regions, precipitation may delay green-up by two possible connections: thicker snowpack and increased cloudiness (Fu et al., 2014b). To include these effects of precipitation on the green-up date, we utilized the 2-month accumulated precipitation before the SOS (Cong et al., 2013; Fu et al., 2014b). The spatial pattern of PR (Fig. 1d) generally exhibits positive correlations over the boreal forests, i.e., increases in PR were related to delayed SOS. This relationship was clear in Scandinavia and Siberia; however, it was relatively weak and shows larger regional variations than in the other climate variables.

2.2. Long-term influence of each climatic variable on SOS trends

We designed a linear model of the SOS to assess the influences of each climate field (i.e., WD, PT, GT, and PR) on the recent change in the SOS trend. The SOS can be represented by a linear combination of the four climate variables with respect to time as follows:

$$\mathrm{SOS(t)} = a_{WD}\, WD(t) + a_{\mathrm{PT}}\, PT(t) + a_{\mathrm{GT}}\, GT(t) + a_{PR}\, PR(t) + \varepsilon(\mathrm{t}) + \mathrm{b}. \tag{5}$$

here, the SOS and the four climate fields are expressed as functions of year (t). The slope coefficients (a_{WD}, a_{PT}, a_{GT}, and a_{PR}) and intercept (b) were trained by multilinear regression using time series of the SOS and the four climate fields at each data point for the entire period. $\varepsilon(t)$ indicates errors that can be related to other climate fields or nonlinearities not accounted for in this approach. By neglecting the error term, the SOS can be approximated by the regressed SOS ($\mathrm{SOS_{reg}}$) as:

$$\mathrm{SOS}_{reg}\,\mathrm{(t)} = a_{WD}\, WD(t) + a_{\mathrm{PT}}\, PT(t) + a_{\mathrm{GT}}\, GT(t) + a_{PR}\, PR(t) + \mathrm{b} \tag{6}$$

$$= I_{WD}(t) + I_{PT}(t) + I_{GT}(t) + I_{PR}(t) + b. \tag{7}$$

The $\mathrm{SOS_{reg}}$ is the linear combination of the four climate fields, representing the changes in the SOS that are driven by these external climate conditions. If the SOS has strong and linear relationships with the four climate fields, two SOS values (the SOS and the $\mathrm{SOS_{reg}}$) will have a high similarity with a small error term. We defined the four terms in Eq. (7) (i.e., I_{WD}, I_{PT}, I_{GT}, and I_{PR}) as the climatic influence terms that are the product of slope coefficients and climatic variables. These influence terms have the same unit as the $\mathrm{SOS_{reg}}$ (i.e., days) and represent the effects of each climate field on the $\mathrm{SOS_{reg}}$. Because the slope coefficients are fixed with whole-year trained values, the $\mathrm{SOS_{reg}}$ and climatic influences do not reflect long-term changes in temperatures or precipitation sensitivity of the SOS.

Based on Eq. (5), the $\mathrm{SOS_{reg}}$ trends (i.e., $\frac{\mathrm{dSOS_{reg}}}{\mathrm{dt}}$) are decomposed into trends of each climatic influence as follows:

$$\frac{\mathrm{dSOS_{reg}}}{\mathrm{dt}} = \frac{dI_{WD}}{dt} + \frac{dI_{PT}}{dt} + \frac{dI_{GT}}{dt} + \frac{dI_{PR}}{dt}. \tag{8}$$

The four terms on the right-hand side of Eq. (8) are the trends of I_{WD}, I_{PT}, I_{GT}, and I_{PR}, which indicate the climatic influences of the WD, PT, GT, and PR, respectively, on the SOS trends for a given location and period.

Using the above equations for the four climatic fields, we decomposed the long-term changes of the $\mathrm{SOS_{reg}}$ into the trends of climatic influences (i.e., $\frac{dI_{WD}}{dt}$, $\frac{dI_{PT}}{dt}$, $\frac{dI_{GT}}{dt}$, and $\frac{dI_{PR}}{dt}$) for the earlier period (1982–1997) and for the entire period (1982–2013). By comparing the

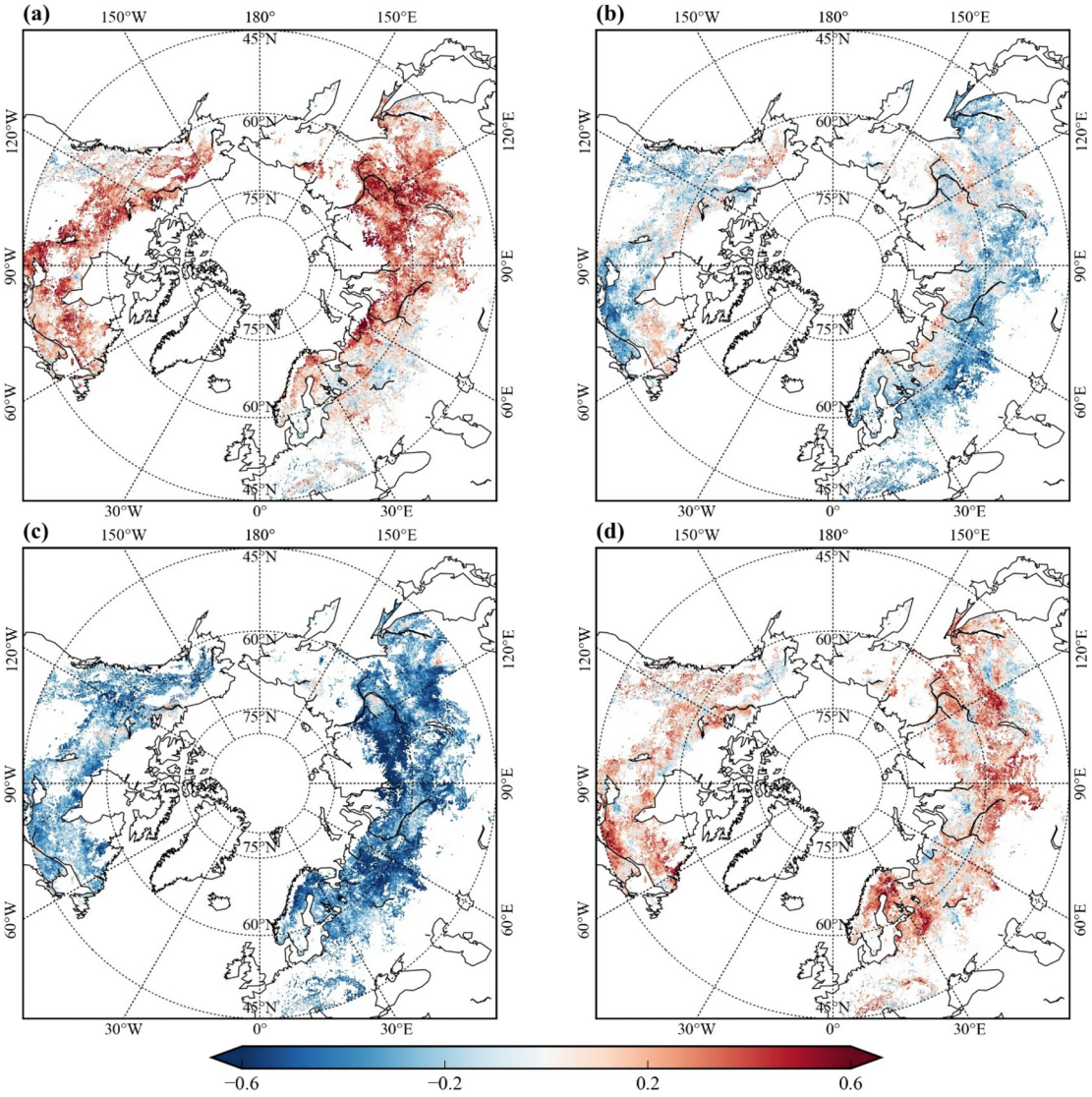

Fig. 1. Spatial distributions of partial correlations between the SOS and (a) WD, (b) PT, (c) GT, and (d) PR during the entire period (1982–2013).

entire period to the earlier period, we can elucidate the slowdown of the SOS trends after the late 1990s and associated mechanisms using the multilinear approach. Wang et al. (2015) reported that a possible turning point of the SOS trends was mostly assigned to the late 1990s, especially 1997, over the regions where the SOS trends were likely to be changed. A changing point analysis using the method of Lund and Reeves (2002) yielded similar results as Wang et al. (2015). Therefore, we selected 1997 as the turning point and the end of the earlier period. Our key findings did not differ with a longer or shorter definition of the earlier period.

Based on this approach, we quantitatively interpreted the climatic factors of the green-up slowdown. Although this method was based on linear assumptions and, therefore, was unable to determine sensitivity changes or nonlinear responses, it is a simple and powerful analysis for clarifying underlying climatic mechanisms of the SOS slowdown in the recent decade.

3. Results

3.1. Weakening of the spring green-up advancement in recent decades

To interpret the green-up slowdown, this study compared the SOS trend for the earlier period to that for the entire period, before presenting the influence of individual climate fields. Fig. 2 displays the spatial patterns of the SOS trend during the earlier and the entire period. During the earlier period (Fig. 2a), the trends were generally negative, indicating advancements of the SOS over the study region (-0.22 ± 0.42 days yr^{-1}). Approximately 70% of the study region showed advancements of the SOS with 18% being statistically significant ($p < 0.05$) over the whole region. This advancing trend was apparent in Siberia and NWNA. In contrast, delaying of the SOS was found in 30% of the entire area and only 7% was statistically significant ($p < 0.05$). These delaying trends mainly appeared over northern Siberia, Scandinavia, and northeastern North America. During the entire period (Fig. 2b), the prevailing trend of earlier green-up was weakened over boreal forests (-0.10 ± 0.26 days yr^{-1}), especially in Siberia and NWNA. The proportion of the negative SOS trends was 70%, with 20% being statistically significant ($p < 0.05$) over the whole region. This percentage was similar to that in the earlier period; however, the region with a strong advancing trend (< -0.3 days yr^{-1}) was about 15% of the study region, less than one half that in the earlier period (36%).

Weakening of the SOS advancing trends corresponded to positive differences between the SOS advancing trends for the earlier period and the entire period (Fig. 2c). From a hemispheric view, the SOS advancement appeared over the boreal forests for the entire period (Fig. 2b); however, its strength was weaker than for the earlier period

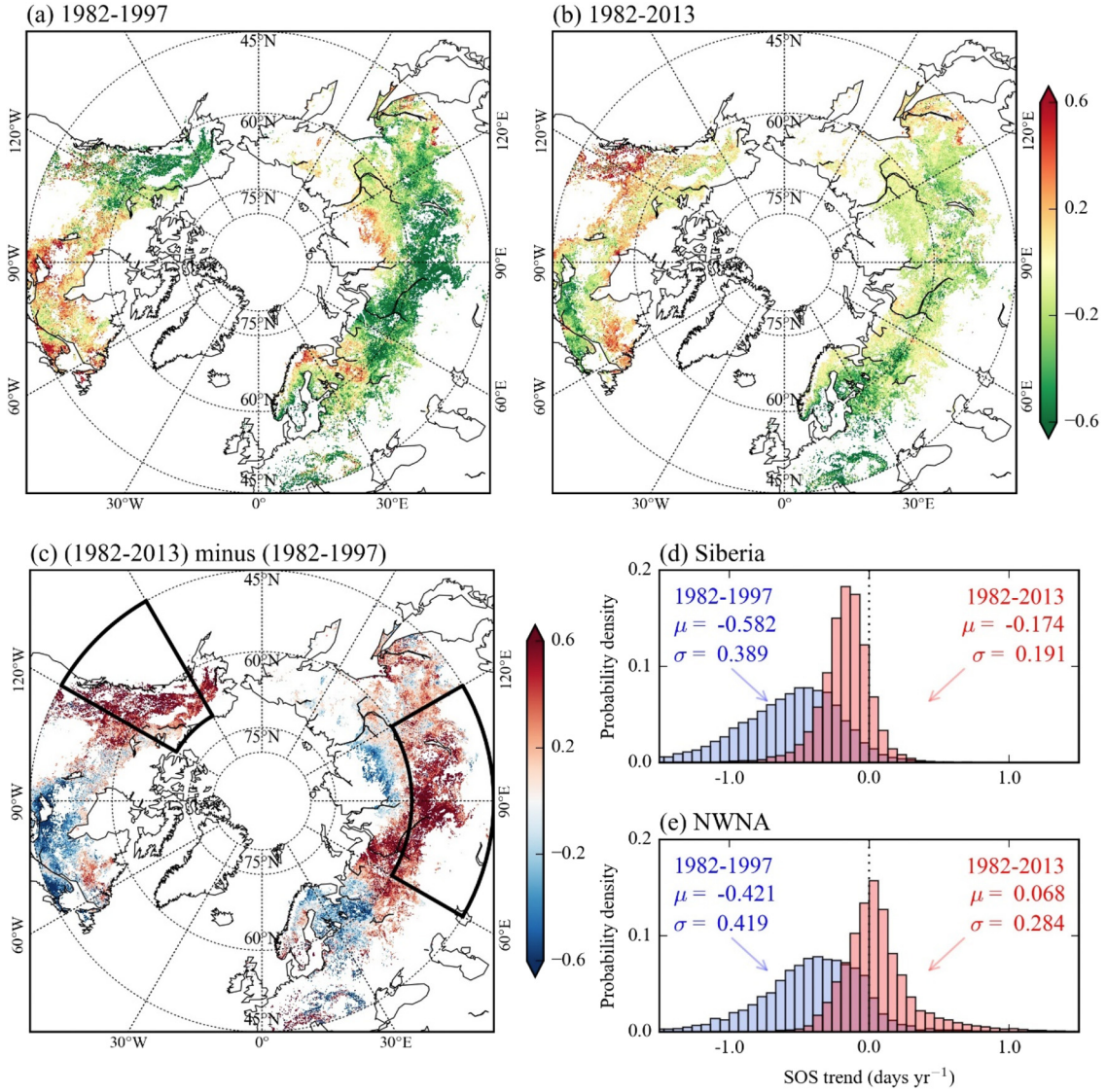

Fig. 2. Spatial patterns of the SOS trends during (a) the earlier period (1982–1997) and (b) the entire period (1982–2013). (c) The difference map between the two periods (1982–2013 minus 1982–1997). Probability density functions of the SOS trends over (d) Siberia (45°N–60°N, 60°E–120°E) and (e) NWNA (45°N–70°N, 120°W–150°W) during the earlier period (blue) and the entire period (red). (For interpretation of the references to color in this figure legend, the reader is referred to the web version of this article.)

(Fig. 2c). In particular, this slowdown of SOS advancing was apparent in the region 45°N–60°N and 60°E–120°E (hereafter Siberia) as well as in 45°N–70°N and 120°W–150°W (hereafter NWNA). Fig. 2d and e show the probability density functions (PDFs) of the SOS trend over Siberia and NWNA for the earlier period and for the entire period. For the earlier period (blue in Fig. 2d and e), the region-averaged SOS trends were -0.58 ± 0.39 days yr^{-1} and -0.42 ± 0.42 days yr^{-1} for Siberia and NWNA, respectively. The PDFs had thick left tails that mean large proportions of forests experienced strong SOS advancing trends in both regions (blue). In contrast, for the entire period (red in Fig. 2d and e), the magnitude of SOS trends decreased in Siberia (-0.17 ± 0.19 days yr^{-1}) and NWNA (0.07 ± 0.28 days yr^{-1}), and the PDFs were much narrower than for the earlier period (red). The regional slowdown of the SOS advancement was consistent with the findings in earlier studies for different regions and periods (Fu et al., 2014a; Jeong et al., 2011; Wang et al., 2015).

This study examined the spatial patterns of the SOS_{reg} trends in the earlier and the entire periods to verify that the multilinear approach is appropriate to understand the recent slowdown of SOS trends over Siberia and NWNA. The general characteristics of the slowdown of the SOS trends were also displayed in the spatial patterns of the SOS_{reg} trends (Fig. 3). Fig. 3a and b show the distribution of the SOS_{reg} trends for the earlier period and for the entire period, respectively. Compared to the SOS trends in Fig. 2, the SOS_{reg} trends tended to be weaker but were similar spatial distributions for both periods. During the earlier period (Fig. 3a), the strong advancing trends in Siberia and NWNA were well represented. For the entire period (Fig. 3b), the slowdown pattern of the SOS trends in Fig. 2b was also found in the SOS_{reg} trend over the study regions, especially in Siberia and NWNA. The difference of the SOS_{reg} trend between these two periods (Fig. 3c) clearly showed the slowdown of the SOS_{reg} trends in Siberia and NWNA similarly as that shown in Fig. 2c. This was relatively weaker than the advancing trends in Scandinavia and the delaying trends in NWNA in Fig. 2; however, the spatial variations of the SOS_{reg} trends agreed closely with the observed patterns of spring phenology trends. In Siberia and NWNA (Fig. 3d and e), the PDFs of the SOS_{reg} trend showed weaker and narrower distributions for the entire period similarly as that shown in Fig. 2d and e. Over Siberia (Fig. 3d), the SOS_{reg} trends were weakened from -0.40 ± 0.30 days yr^{-1} for the earlier period to -0.16 ± 0.10 days yr^{-1} for the entire period. These SOS_{reg} trends

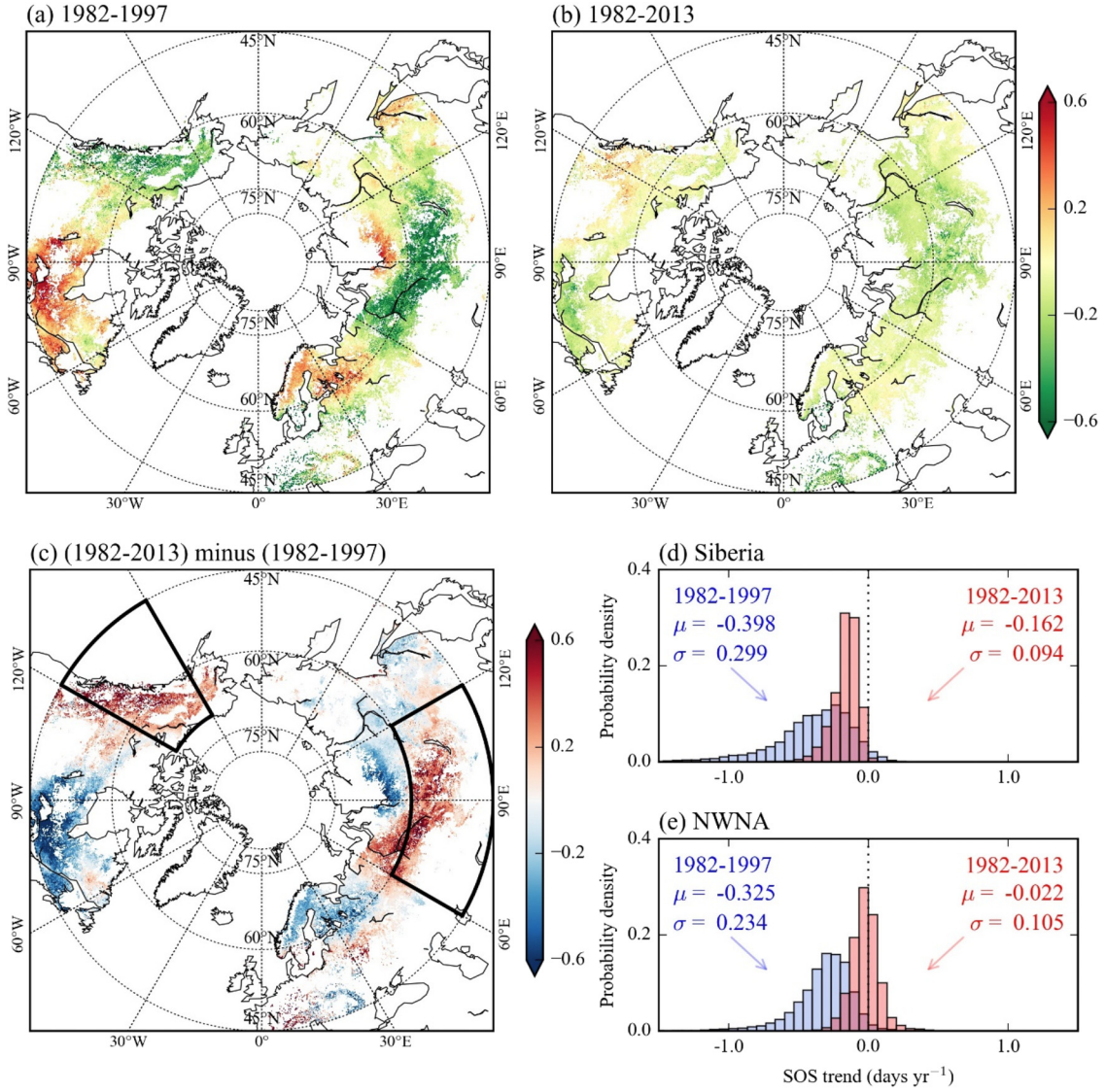

Fig. 3. Same as in Fig. 2 except for the SOS_{reg} trends.

were relatively weak compared to the SOS trends, -0.58 ± 0.39 days yr^{-1} for the earlier period and -0.17 ± 0.19 days yr^{-1} for the entire period (Fig. 2d). The ratio of the SOS_{reg} trend to the SOS trend increased from 68% for the earlier period to 93% for the entire period. This indicates that SOS_{reg} explained the SOS trends particularly well for the entire period. Over NWNA (Fig. 3e), the SOS_{reg} trends changed from -0.33 ± 0.23 days yr^{-1} during the earlier period to -0.02 ± 0.11 days yr^{-1} during the entire period (from -0.42 ± 0.42 days yr^{-1} during the earlier period to 0.07 ± 0.28 days yr^{-1} during the entire period for the SOS trends). The ratio of the SOS_{reg} trend to the SOS trend was 75% during the earlier period; for the entire period, both the SOS and SOS_{reg} trends were near zero with opposite signs to each other. Compared to the earlier period, magnitude of the SOS_{reg} trends decreased by 0.24 and 0.31 days yr^{-1} in Siberia and NWNA, respectively, for the entire period. This was relatively small compared to the differences in the actual SOS trends (0.41 and 0.49 days yr^{-1}, respectively). However, the differences in the SOS_{reg} trend explained over 50% of the differences from the SOS trend for both regions.

These results revealed that the SOS_{reg}, which is composed of the trends of the four climate fields (i.e., the trend of I_{WD}, I_{PT}, I_{GT}, and I_{PR}) can represent the general characteristics of the slowdown of green-up advancement trends, especially in Siberia and NWNA. Based on this linear-regression approach, we investigated the I_{WD}, I_{PT}, I_{GT}, and I_{PR} trends during the earlier period and the entire period to clarify the main factor of the slowdown of the SOS trends over the boreal forests.

3.2. The major factor of the weakening spring green-up advancements

Based on the multilinear regression, the SOS_{reg} trends during the earlier period and the entire period (Fig. 3a and b) were decomposed into the trends of the four climatic influences, i.e., $\frac{dI_{WD}}{dt}$, $\frac{dI_{PT}}{dt}$, $\frac{dI_{GT}}{dt}$, and $\frac{dI_{PR}}{dt}$ (Fig. 4). In Fig. 4, positive trends of I_{WD}, I_{PT}, I_{GT}, and I_{PR} were interpreted as a delaying effect of the SOS trends affected by the lengthening of WD, cooling of PT, cooling of GT, and increase of PR, respectively, and vice versa. As mentioned previously, this approach does not consider any changes in the SOS sensitivity to temperatures or precipitation with time because the regression coefficients are stationary (i.e., time-invariant).

Fig. 4a–d show the spatial distributions of I_{WD}, I_{PT}, I_{GT}, and I_{PR} trends during the earlier period, respectively. These distributions were similar to the patterns of SOS_{reg} trends (Fig. 3a) because the SOS_{reg} is the sum of trends of climatic influences; however, the detailed features vary for the different variables and it gives information about relative importance of each climate field. The strong negative trends in Siberia

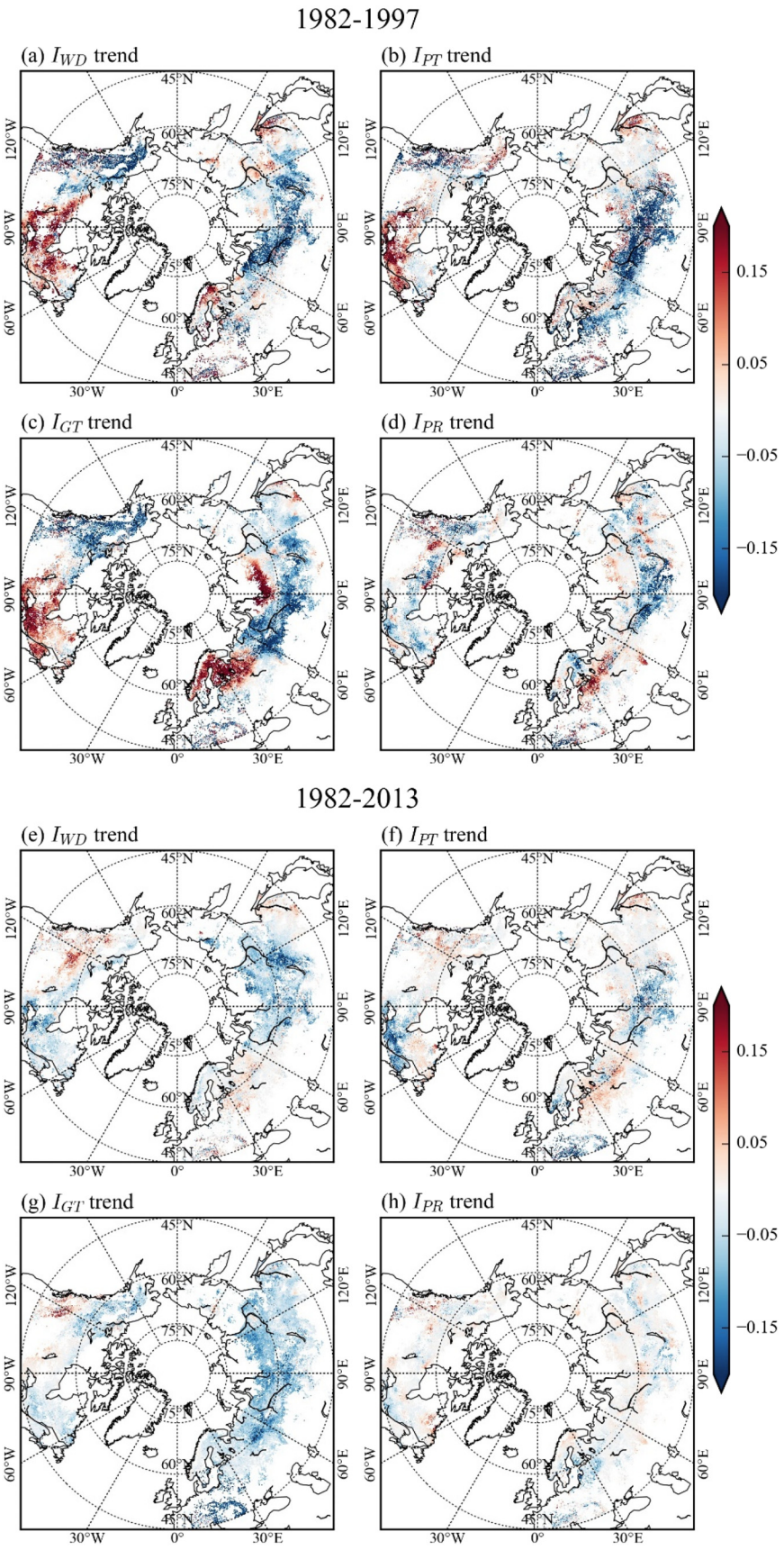

Fig. 4. Spatial distributions of the (a, e) I_{WD}, (b, f) I_{PT}, (c, g) I_{GT}, and (d, h) I_{PR} trends on the SOS trends during the earlier period (1982–1997) and the entire period (1982–2013).

in Fig. 3a commonly appear in the I_{WD}, I_{PT}, I_{GT}, and I_{PR} trends (Fig. 4a–d). The negative trends around Siberia imply that the climate influences acted toward the advancing trends of SOS_{reg} in this region. Contrary to Siberia, the I_{WD} and I_{GT} trends showed large negative values in NWNA (Fig. 4a and c); however, the I_{PT} and I_{PR} values were relatively small, i.e., strong earlier SOS_{reg} trends in NWNA were mainly associated with the I_{WD} and I_{GT} trends during the earlier period. In northeastern North America, the delaying trends of SOS_{reg} (Fig. 3a) were also explained by a combination of the positive trends of I_{WD}, I_{PT}, and I_{GT}. Positive effects of I_{GT} trends (Fig. 4c) on the SOS_{reg} trends were distinct in northern Siberia and Scandinavia; these effects were not found in the other three parameters. Therefore, the positive SOS_{reg} trends in these regions (Fig. 3a) were connected to the localized positive I_{GT} trend, i.e., delayed by the temperature decreases around the GT period. The I_{PR} trends (Fig. 4d) showed regionally confined but strongly negative influences around Siberia. However, the I_{PR} trends did not exhibit distinct effects in other regions compared to the I_{WD}, I_{PT}, and I_{GT} trends. These results showed that the I_{WD}, I_{PT}, and I_{GT} trends mainly contributed to the strong advancing trends of the SOS_{reg} over the boreal forests during the earlier period (Fig. 4a–d).

For the entire period (Fig. 4e–h), the magnitude of I_{WD}, I_{PT}, I_{GT}, and I_{PR} trends decreased over the study region, consistently with the SOS_{reg} trends (Fig. 3b). In Siberia, the region of apparent slowdown in the SOS_{reg} trends, the trends of I_{WD}, I_{PT}, and I_{GT} were negative (Fig. 4e–g); however, their magnitudes were relatively smaller than those during the earlier period. Similarly, in NWNA, the magnitudes of I_{WD} and I_{GT} trends were notably smaller (Fig. 4e and g) than the strong negative trends during the earlier period (Fig. 4a and c). In northeastern North America, the clear positive trends in Fig. 4a–c changed to relatively weak negative trends for the entire period (Fig. 4e–g) and the trend of I_{GT} was relatively larger than the trend of other terms. The I_{PR} trend decreased to near zero and almost disappeared in the northern boreal forests (Fig. 4h), i.e., the long-term effects of precipitation on the SOS_{reg} trend are negligible.

To understand the time evolution of the SOS slowdown and associated climatic mechanism in Siberia and NWNA, we examined the trends of the SOS, SOS_{reg}, I_{WD}, I_{PT}, I_{GT}, and I_{PR} over five different periods: the earlier period and the entire period with three intermediate periods between 1982 and 2001, 1982 and 2005, and 1982 and 2009 (Fig. 5). In Siberia for the earlier period, the SOS_{reg} trend (i.e., the sum of I_{WD}, I_{PT}, I_{GT}, and I_{PR} trends) was -0.38 days yr^{-1} and the trends of I_{WD}, I_{PT}, I_{GT}, and I_{PR} were -0.10, -0.11, -0.11, and -0.06 days yr^{-1}, respectively (Fig. 5a). The SOS trend was -0.57 days yr^{-1} and 67% of the SOS trends can be explained by the SOS_{reg} trends. For the other four periods, the SOS trends gradually decreased with time, with the SOS_{reg} trends representing this weakening of the SOS trends well. The decreased SOS_{reg} trend indicates that the trends of climate fields were reduced. The magnitudes of I_{WD} and I_{PT} trends were reduced to less than half of it in the earlier period to the entire period. During the two intermediate periods (1982–2001 and 1982–2005), the I_{GT} trends were strengthened and remained greater than half of the SOS_{reg} trends. This shows that the GT exerted strong impacts on the SOS trends over Siberia until 2005. However, similar to the remaining fields, the strong I_{GT} trends decreased after 2005 to result in the slowdown of the SOS trends. Over the entire period, the trends of I_{WD}, I_{PT}, I_{GT}, and I_{PR} were -0.06, -0.03, -0.06, and 0.00 days yr^{-1}, respectively. All these trends decreased to about half of those for 1982–1997 (-0.10, -0.11, -0.11, and -0.06 days yr^{-1}, respectively) and the SOS_{reg} trend decreased from -0.38 days yr^{-1} for the earlier period to -0.16 days yr^{-1} for the entire period. This weakening consistently appeared in the SOS trend, i.e., approximately -0.16 days yr^{-1} in the entire period and only one-third of -0.57 days yr^{-1} in the earlier period. These results indicate that the weakened SOS trends over Siberia were influenced by simultaneous weakening of the I_{WD}, I_{PT}, and I_{GT} trends.

Time series of the SOS, SOS_{reg}, WD, PT, and GT (Fig. 5c) showed similar characteristics as in Fig. 5a. In Siberia, the changes in regional averaged SOS and SOS_{reg} showed quite similar interannual variations (correlation coefficient, $r = 0.91$) and a weakening trend with increasing time. The strong advancing trends of the earlier period coincided with the WD minimum and PT maximum in 1997. Regardless of 1997, the strong advancing trends for SOS and SOS_{reg} were attributed to GT increases in Siberia until 2005. After 2005, the GT rapidly decreased to the level of the 1980s to result in the slowdown of SOS_{reg} trends in Siberia. Therefore, the weakened SOS_{reg} trend in Siberia was closely related to the GT, indicating temperature conditions during the green-up period, rather than the other climate fields.

Slowdown of the SOS_{reg} trends over NWNA similarly occurred; however, details were different from over Siberia (Fig. 5b). During the earlier period, the I_{WD}, I_{PT}, I_{GT}, and I_{PR} trends were -0.14, -0.02, -0.11, and -0.02 days yr^{-1}, respectively, and the SOS_{reg} was 0.30 days yr^{-1}. The SOS trend was approximately -0.40 days yr^{-1}, equivalent to 75% of the SOS_{reg} trend. The I_{WD} and I_{GT} trends comprised most of the SOS_{reg} trends (47% and 37%, respectively) over NWNA during the earlier period. The magnitudes of SOS and SOS_{reg} trends were substantially weakened with time, which was concurrent with the decreases in the I_{WD} and I_{GT} trends. The SOS trend was approximately 0.03 days yr^{-1} for the entire period, which contrasted the strong advancing trends during the earlier period (-0.40 days yr^{-1}). The SOS_{reg} was approximately -0.03 days yr^{-1} and decomposed to -0.00, 0.01, -0.04, and -0.00 days yr^{-1} for the I_{WD}, I_{PT}, I_{GT}, and I_{PR} trends, respectively. The magnitude of the SOS_{reg} trend was weakened with the SOS trend similarly for the entire period; however, it cannot represent the reversed sign of the SOS trends.

The slowdown of the green-up trends in NWNA was apparent (Fig. 5d). Both the SOS and the SOS_{reg} showed strong negative trends affected by the WD and GT trends until the early 2000s (Fig. 5b). After early 2000s, the trends of WD and GT were severely reduced, and this weakening led to the slowdown of the SOS trends over NWNA. The SOS_{reg} captured the interannual variations in the SOS in NWNA ($r = 0.84$) well; however, it was slightly smaller than that in Siberia ($r = 0.91$). This intercontinental difference can be found the spatial pattern of coefficient of determination (Fig. 6). This relatively weaker correlation originated from mismatches between the SOS and SOS_{reg} after 2010. From 2010, the SOS and the SOS_{reg} showed differences greater than five days and these differences result in the opposite sign of the SOS_{reg} trend during the entire period. These gaps between the SOS and SOS_{reg} cannot be represented by the linear approach used in the present study.

4. Conclusion

There is a general expectation that the spring phenology will advance with global warming, especially over boreal forests that are strongly affected by temperatures (Garonna et al., 2016; Melaas et al., 2016; Richardson et al., 2013). Contrary to this common perception, this study shows there has been a slowdown of the SOS advancement over the NH boreal forests since the late 1990s (Fig. 2). Considering the complicated nature of spring phenology, this slowdown may have been affected by either the changes in external climate conditions, e.g., weakened spring warming (Jeong et al., 2011) or by adjustments of the internal sensitivity, e.g., increased heat requirement by lost chilling (Fu et al., 2015). This study has analyzed the climate fields related to the spring phenology over the boreal forests to identify the key processes contributing to the green-up slowdown. Note that the present study does not consider any changes in sensitivity. Overall, features of the green-up slowdown (Fig. 2) could be reproduced by the SOS_{reg} (Fig. 3), which is the linear combination of the WD, PT, GT, and PR. Though the SOS_{reg} trends are relatively weaker than the SOS trends, it suggests that the green-up slowdown was largely influenced by these external climatic factors, rather than the changes in internal sensitivity. We decomposed the SOS_{reg} trends into the I_{WD}, I_{PT}, I_{GT}, and I_{PR} trends to investigate the relative importance of each factor that influenced on the

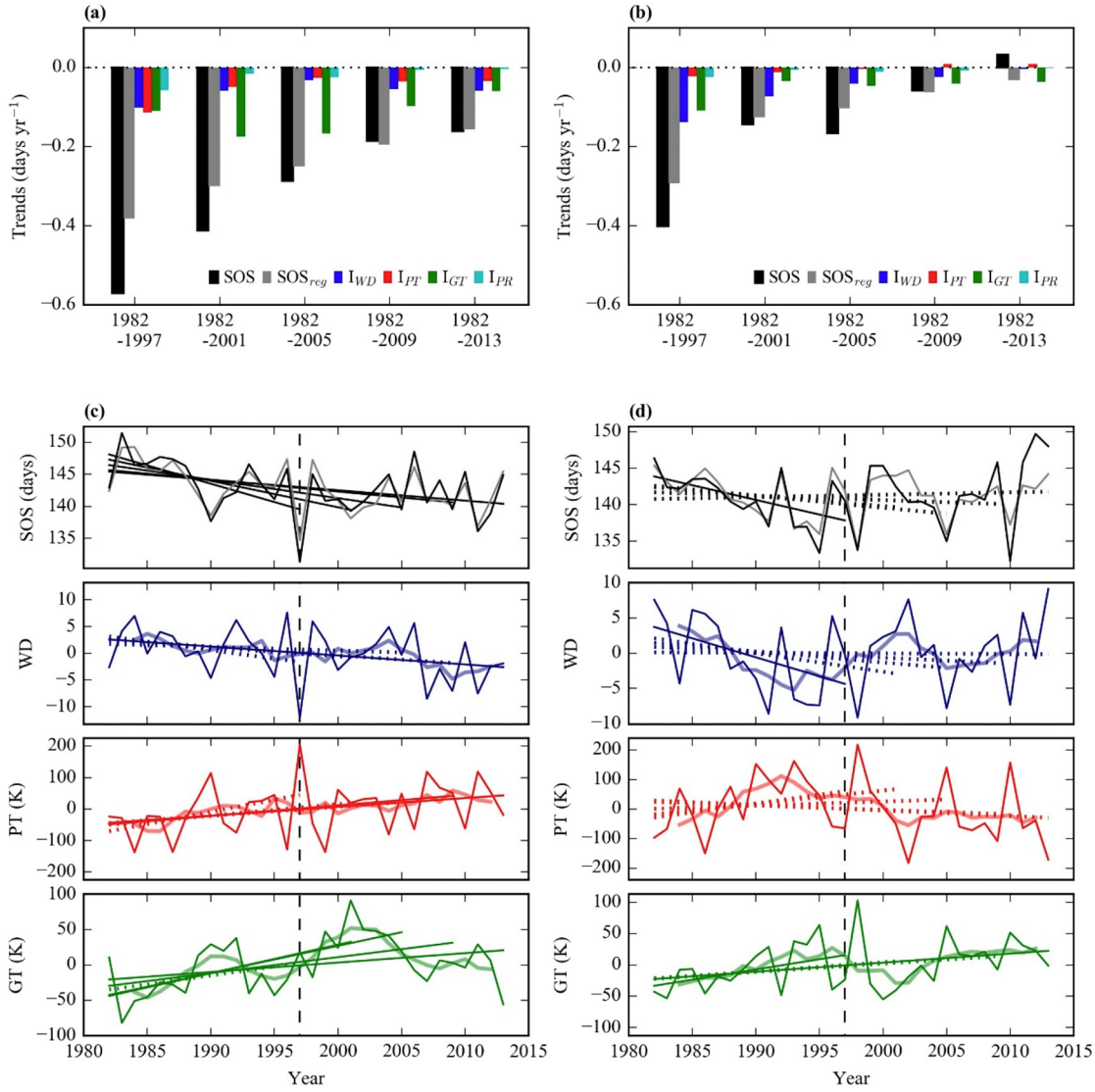

Fig. 5. Long-term changes in SOS and climatic fields over (a, c) Siberia (45°N–60°N, 60°E–120°E) and (b, d) NWNA (45°N–70°N, 120°W–50°W). (a, b) Changes in long-term trends of the SOS (black), SOS_{reg} (gray), I_{WD} (blue), I_{PT} (red), I_{GT} (green), and I_{PR} (cyan) from 1982 to 1997, 2001, 2005, 2009, and 2013. (c, d) Time series of the SOS (black) and SOS_{reg} (gray) with GT (green), PT (red), and WD (blue) anomalies for the entire period (1982–2013). Linear trends denoted by solid ($p < 0.1$) and dashed ($p > 0.1$) lines. (For interpretation of the references to color in this figure legend, the reader is referred to the web version of this article.)

green-up slowdown, which was apparent over Siberia and NWNA (Figs. 4 and 5). In Siberia, the strong advancing trends of SOS was attributed to the I_{GT} trends; however, it was severely decreased after the early 2000s (Fig. 5a and c). In NWNA, the SOS trend was affected by the I_{WD} and I_{GT} trends until the late 1990s; however, the trends of I_{WD} and I_{GT} were reduced with time to result in the weakening of the SOS advancing trends in the earlier period (Fig. 5b and d). These results show that the weakening of the warming trend largely contributed to the green-up slowdown in Siberia and NWNA after the early 2000s.

This weakening of warming trends in Siberia and NWNA coincides with the global warming hiatus, the period for which the global-mean surface temperature barely increased or even decreased after early 2000s (Kosaka and Xie, 2013; Meehl et al., 2011). In this period, the magnitude of spring warming decreased to one half of that in the preceding decades; even the winter temperature in the 1990s are lower than that in the 1980s (Li et al., 2015). There are intense debates about the warming hiatus and related mechanisms from the global (Gleisner et al., 2015; Karl et al., 2015; Kosaka and Xie, 2013; Meehl et al., 2011) and regional perspectives (Kug et al., 2015; Wang et al., 2017). Nonetheless, the weakening of spring warming trends is observed in high-latitude regions (Jeong et al., 2011; Wang et al., 2015). This study shows that this slowdown (or weakening) of warming trends in the recent decade is likely the primary factor of the slowdown of the advancing trend in the spring green-up. It also implies that if the spring temperatures in boreal forests start increasing again, the advancement of the SOS will resume like in the early 2000s. Global warming is expected to continue with persistent anthropogenic greenhouse gas emissions in the near future for over multi-decadal time scales (Kosaka and Xie, 2013; Meehl et al., 2011). This study suggests that the advancing trend of spring phenology will continue in boreal forests in the near future.

Results from this study emphasize the importance of overall intraseasonal warming patterns on SOS changes. The GT, the mean temperature in the 30 days around the green-up date, strongly influenced the SOS trends over not only Siberia and NWNA but also over vast boreal forests during the recent three decades (Figs. 4 and 5). The WD and PT should also be considered to understand the detailed characteristics of the long-term SOS trends. The strong SOS advancement over Siberia in the earlier period (Fig. 2a) cannot be explained without an association among WD, PT, and GT (Fig. 4a–c). The SOS-

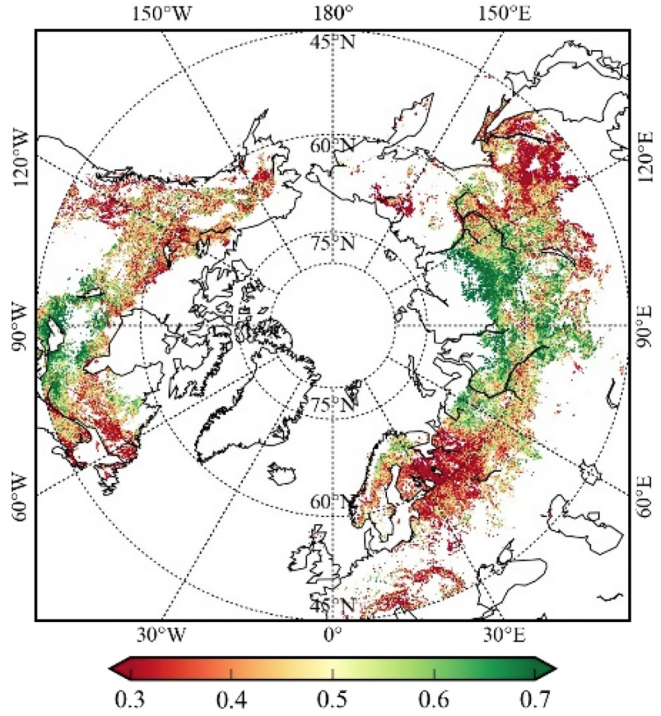

Fig. 6. Spatial distribution of determination coefficient (r^2) between the SOS and SOS_{reg} during the entire period (1982–2013).

delaying trends that are regionally confined to Scandinavia and northern Siberia during the earlier period (Fig. 2a) are connected solely to the I_{GT} trend (Fig. 4c). The SOS advancement over Northeastern part of North America during the entire period (Fig. 2b) is mostly involved with the I_{PT} trend pattern (Fig. 4f). These complex contribute on the advancing- or delaying-SOS trends imply that we should consider the entire pattern of intraseasonal warming from winter to green-up to understand the SOS trend precisely. In contrast, the influence of PR is negligible compared to the other temperature field especially for the entire period (Fig. 4h); this suggests that PR does not play a critical role on the long-term SOS trends in spite of its modest interannual correlations (Fig. 1d).

Satellite-retrieved datasets are useful for examining wide regions of interest; however, careful attention must be paid to their uncertainties and weaknesses in determining the SOS. We utilized the GIMMS $NDVI_{3g}$ dataset in conjunction with the logistic curve fitting method to obtain the SOS in boreal forests in this study. High-latitude vegetation can also be affected by snow; GIMMS $NDVI_{3g}$ prevents the snow effect by using average seasonal profiles or spline interpolations (Garonna et al., 2016; Pinzon and Tucker, 2014). In addition, all negative NDVI values were excluded to avoid the snow contamination problem. The logistic fitting method has been applied considering that it has been found to be appropriate for describing the NDVI transition from winter to summer in high-latitude regions (Beck et al., 2006; Julien and Sobrino, 2009; Zhang et al., 2003). A perfect method for identifying SOS from satellite data remains to be established (Atkinson et al., 2012; Garonna et al., 2016). A number of other methods such as harmonic analysis (Cong et al., 2013), polynomial fitting (Jeong et al., 2011), or logistic fitting (Park et al., 2015) have also been employed for smoothing NDVIs and for retrieving the SOS in other studies. Differences among these methods can be a source of uncertainties in obtaining the SOS and its trends (Atkinson et al., 2012; Cong et al., 2013). We plan to examine the uncertainties in satellite-based SOS determination in high-latitude forests in future studies to follow.

This study shows notable differences between Siberia and NWNA. Most of the temporal changes of the SOS in Siberia (Fig. 5c) can be explained by the multilinear regression model with high correlation coefficient of 0.91. This high correlation suggests that the SOS in the Siberian boreal forests is strongly and linearly linked to climate conditions. Therefore, at least in this climate regime, the Siberian forests are likely to experience the SOS advancement with regional warming. However, in NWNA, there is a mismatch between the SOS and the SOS_{reg} after 2010 (Fig. 5d) with smaller correlation coefficient by 0.84 compared to Siberia. For NWNA, the multilinear approach cannot fully describe the delaying trend of the SOS for the entire period, and this gap comes from higher SOS values after 2010 than in the earlier period. This limitation of the multilinear approach may be related to the changes in external climate conditions, nonlinear sensitivity of spring phenology, or ecological drivers, or some combinations of these factors, which are not considered in this study.

Firstly, this study does not take into account other climate variables such as insolation or photoperiod. Insolation is so highly correlated with temperatures that we did not include it in the regression model to avoid collinearity problem. Also, photoperiod is not a major constraining factor on spring phenological events in the present-day climate conditions (Way and Montgomery, 2014). Though temperature plays the primary role in spring phenology (Hänninen and Kramer, 2007), we cannot rule out the possibility that other climate variables such as insolation, photoperiod, daytime and/or nocturnal temperatures also affected the changes in spring phenology (Cannell and Smith, 1983; Cook et al., 2012; Fu et al., 2014b; Fu et al., 2015; Laube et al., 2014; Melaas et al., 2016; Rossi and Isabel, 2017).

Another possibility is the nonlinearity in vegetation physiology which can affect the sensitivity of spring phenology to temperature. WD, defined as the number of freezing days, is a factor that can hinder the green-up process by either a cold environment or lingering snowpack in the high-latitude regions. However, decreases in WD can suppress vegetation growth by lost chilling mechanism, increasing the required heat amount for spring phenology by decreasing the coldness exposure (Fu et al., 2015; Laube et al., 2014; Melaas et al., 2016). Despite their potential importance, the multilinear approach cannot represent this lost chilling mechanism because the regression coefficients are fixed as a constant. In addition, the change in optimal preseason for spring phenology is a possible nonlinear mechanism which can adversely affect model performance in NWNA. Warming makes the length of optimal preseason shorter, and it can result in the reduction of the apparent temperature sensitivity (Güsewell et al., 2017). Our approach is based on fixed preseason windows (i.e., PT definition) which cannot take into account the changes in optimal preseason or the temporal changes in temperature sensitivity. The optimal preseason varies widely among species (Güsewell et al., 2017) and is hard to define it precisely in the large-scale phenology. It is noted that the nonlinearity should be considered to understand the dynamics of spring phenology in terms of external climate conditions.

Furthermore, other ecological drivers such as wildfire, insect outbreak, and succession can influence mismatches between the SOS and the SOS_{reg} as their effects cannot be explained by a multilinear approach. Fire and/or insect occurrence hinders vegetation activities and further changes the forest characteristics via succession and species composition (McCullough et al., 1998; Schoennagel et al., 2017). Additionally, previous studies showed that the North American boreal forests tend to show more distinct NDVI drops and fast recovery after fire disturbances compared to the Eurasian forests (Beck and Goetz, 2011). This intercontinental difference in the post-fire vegetation recovery or other ecological traits could have induced the differences between Siberia and NWNA shown in Fig. 5.

Considering relatively lower correlation in NWNA, the effects of these internal and external drivers not considered in this study in NWNA may be larger than in Siberia. It implies that considering temperatures solely within a framework of linear modeling may not be sufficient for predicting future phenological changes, especially for the NWNA boreal forest. Further studies are needed to understand the

regional differences between Siberia and NWNA based not only on satellite-retrieved data but also on in-situ observations through various viewpoints from the external climate conditions to the internal or ecological drivers.

This study demonstrates that the recent slowdown of the green-up date advancement in boreal forests is largely attributed to the weakened warming on the basis of the multilinear approach and satellite-retrieved NDVI. Without considering the changes in the internal sensitivity, the changes in the external forcing including the freezing days and the temperatures in the preseason/green-up period, explain much of the variations in the spring phenology, especially in Siberia. The slowdown of the spring phenology in boreal forests is likely a temporary event; significant SOS advancement will be resumed when temperatures start to rise in the near future. Our findings suggest that the green-up date of boreal forests should be examined and monitored continuously to understand the nature and the future of terrestrial ecosystems.

Acknowledgements

This study was funded by the Korea Ministry of Environment (MOE) as a part of the Climate Change Correspondence Program. Su-Jong Jeong was supported by the Korea Meteorological Administration Research and Development Program under Grant KMI (KMI2018-03711) and Jinwon Kim was partially supported by the NIMS/KMA (NIMS-2016-3100).

References

Atkinson, P.M., Jeganathan, C., Dash, J., Atzberger, C., 2012. Inter-comparison of four models for smoothing satellite sensor time-series data to estimate vegetation phenology. Remote Sens. Environ. 123, 400–417. https://doi.org/10.1016/j.rse.2012.04.001.

Badeck, F.-W., Bondeau, A., Böttcher, K., Doktor, D., Lucht, W., Schaber, J., Sitch, S., 2004. Responses of spring phenology to climate change. New Phytol. 162, 295–309. https://doi.org/10.1111/j.1469-8137.2004.01059.x.

Barichivich, J., Briffa, K.R., Myneni, R.B., Osborn, T.J., Melvin, T.M., Ciais, P., Piao, S., Tucker, C., 2013. Large-scale variations in the vegetation growing season and annual cycle of atmospheric CO_2 at high northern latitudes from 1950 to 2011. Glob. Chang. Biol. 19, 3167–3183. https://doi.org/10.1111/gcb.12283.

Bastos, A., Ciais, P., Park, T., Zscheischler, J., Yue, C., Barichivich, J., Myneni, R.B., Peng, S., Piao, S., Zhu, Z., 2017. Was the extreme Northern Hemisphere greening in 2015 predictable? Environ. Res. Lett. 12, 044016. https://doi.org/10.1088/1748-9326/aa67b5.

Beck, P.S.A., Goetz, S.J., 2011. Satellite observations of high northern latitude vegetation productivity changes between 1982 and 2008: ecological variability and regional differences. Environ. Res. Lett. 6, 045501. https://doi.org/10.1088/1748-9326/6/4/045501.

Beck, P.S.A., Atzberger, C., Høgda, K.A., Johansen, B., Skidmore, A.K., 2006. Improved monitoring of vegetation dynamics at very high latitudes: a new method using MODIS NDVI. Remote Sens. Environ. 100, 321–334. https://doi.org/10.1016/j.rse.2005.10.021.

Bonan, G.B., 2008. Forests and climate change: forcings, feedbacks, and the climate benefits of forests. Science 320, 1444–1449. https://doi.org/10.1126/science.1155121.

Cannell, M.G.R., Smith, R.I., 1983. Thermal time, chill days and prediction of budburst in *Picea sitchensis*. J. Appl. Ecol. 20, 951–963. https://doi.org/10.2307/2403139.

Cong, N., Wang, T., Nan, H., Ma, Y., Wang, X., Myneni, R.B., Piao, S., 2013. Changes in satellite-derived spring vegetation green-up date and its linkage to climate in China from 1982 to 2010: a multimethod analysis. Glob. Chang. Biol. 19, 881–891. https://doi.org/10.1111/gcb.12077.

Cook, B.I., Wolkovich, E.M., Parmesan, C., 2012. Divergent responses to spring and winter warming drive community level flowering trends. PNAS 109, 9000–9005. https://doi.org/10.1073/pnas.1118364109.

de Jong, R., Verbesselt, J., Zeileis, A., Schaepman, M.E., 2013. Shifts in global vegetation activity trends. Remote Sens. 5, 1117–1133. https://doi.org/10.3390/rs5031117.

Dee, D.P., Uppala, S.M., Simmons, A.J., Berrisford, P., Poli, P., Kobayashi, S., Andrae, U., Balmaseda, M.A., Balsamo, G., Bauer, P., Bechtold, P., Beljaars, A.C.M., van de Berg, L., Bidlot, J., Bormann, N., Delsol, C., Dragani, R., Fuentes, M., Geer, A.J., Haimberger, L., Healy, S.B., Hersbach, H., Hólm, E.V., Isaksen, L., Kållberg, P., Köhler, M., Matricardi, M., McNally, A.P., Monge-Sanz, B.M., Morcrette, J.-J., Park, B.-K., Peubey, C., de Rosnay, P., Tavolato, C., Thépaut, J.-N., Vitart, F., 2011. The ERA-Interim reanalysis: configuration and performance of the data assimilation system. Q. J. R. Meteorol. Soc. 137, 553–597. https://doi.org/10.1002/qj.828.

Delbart, N., Le Toan, T., Kergoat, L., Fedotova, V., 2006. Remote sensing of spring phenology in boreal regions: a free of snow-effect method using NOAA-AVHRR and SPOT-VGT data (1982–2004). Remote Sens. Environ. 101, 52–62. https://doi.org/10.1016/j.rse.2005.11.012.

Fu, Y.H., Piao, S., Op de Beeck, M., Cong, N., Zhao, H., Zhang, Y., Menzel, A., Janssens, I.A., 2014a. Recent spring phenology shifts in western Central Europe based on multiscale observations. Glob. Ecol. Biogeogr. 23, 1255–1263. https://doi.org/10.1111/geb.12210.

Fu, Y.H., Piao, S., Zhao, H., Jeong, S.-J., Wang, X., Vitasse, Y., Ciais, P., Janssens, I.A., 2014b. Unexpected role of winter precipitation in determining heat requirement for spring vegetation green-up at northern middle and high latitudes. Glob. Chang. Biol. 20, 3743–3755. https://doi.org/10.1111/gcb.12610.

Fu, Y.H., Zhao, H., Piao, S., Peaucelle, M., Peng, S., Zhou, G., Ciais, P., Huang, M., Menzel, A., Peñuelas, J., Song, Y., Vitasse, Y., Zeng, Z., Janssens, I.A., 2015. Declining global warming effects on the phenology of spring leaf unfolding. Nature 526, 104–107. https://doi.org/10.1038/nature15402.

Garonna, I., de Jong, R., Schaepman, M.E., 2016. Variability and evolution of global land surface phenology over the past three decades (1982–2012). Glob. Chang. Biol. 22, 1456–1468. https://doi.org/10.1111/gcb.13168.

Gleisner, H., Thejll, P., Christiansen, B., Nielsen, J.K., 2015. Recent global warming hiatus dominated by low-latitude temperature trends in surface and troposphere data. Geophys. Res. Lett. 42, 2014GL062596. https://doi.org/10.1002/2014GL062596.

Güsewell, S., Furrer, R., Gehrig, R., Pietragalla, B., 2017. Changes in temperature sensitivity of spring phenology with recent climate warming in Switzerland are related to shifts of the preseason. Glob. Chang. Biol. 23, 5189–5202. https://doi.org/10.1111/gcb.13781.

Hänninen, H., Kramer, K., 2007. A Framework for Modelling the Annual Cycle of Trees in Boreal and Temperate Regions.

Hansen, M.C., Defries, R.S., Townshend, J.R.G., Sohlberg, R., 2000. Global land cover classification at 1 km spatial resolution using a classification tree approach. Int. J. Remote Sens. 21, 1331–1364. https://doi.org/10.1080/014311600210209.

Ho, C.-H., Lee, E.-J., Lee, I., Jeong, S.-J., 2006. Earlier spring in Seoul, Korea. Int. J. Climatol. 26, 2117–2127.

Jeong, S.-J., Ho, C.-H., Jeong, J.-H., 2009. Increase in vegetation greenness and decrease in springtime warming over east Asia. Geophys. Res. Lett. 36, L02710. https://doi.org/10.1029/2008GL036583.

Jeong, S.-J., Ho, C.-H., Gim, H.-J., Brown, M.E., 2011. Phenology shifts at start vs. end of growing season in temperate vegetation over the Northern Hemisphere for the period 1982–2008. Glob. Chang. Biol. 17, 2385–2399. https://doi.org/10.1111/j.1365-2486.2011.02397.x.

Julien, Y., Sobrino, J.A., 2009. Global land surface phenology trends from GIMMS database. Int. J. Remote Sens. 30, 3495–3513. https://doi.org/10.1080/01431160802562255.

Karl, T.R., Arguez, A., Huang, B., Lawrimore, J.H., McMahon, J.R., Menne, M.J., Peterson, T.C., Vose, R.S., Zhang, H.-M., 2015. Possible artifacts of data biases in the recent global surface warming hiatus. Science 348 (80-.), 1469–1472. https://doi.org/10.1126/science.aaa5632.

Keenan, T.F., Gray, J., Friedl, M.A., Toomey, M., Bohrer, G., Hollinger, D.Y., Munger, J.W., O'Keefe, J., Schmid, H.P., Wing, I.S., Yang, B., Richardson, A.D., 2014. Net carbon uptake has increased through warming-induced changes in temperate forest phenology. Nat. Clim. Chang. 4, 598–604. https://doi.org/10.1038/nclimate2253.

Kosaka, Y., Xie, S.-P., 2013. Recent global-warming hiatus tied to equatorial Pacific surface cooling. Nature 501, 403–407. https://doi.org/10.1038/nature12534.

Kug, J.-S., Jeong, J.-H., Jang, Y.-S., Kim, B.-M., Folland, C.K., Min, S.-K., Son, S.-W., 2015. Two distinct influences of Arctic warming on cold winters over North America and East Asia. Nat. Geosci. 8, 759–762. https://doi.org/10.1038/ngeo2517.

Laube, J., Sparks, T.H., Estrella, N., Höfler, J., Ankerst, D.P., Menzel, A., 2014. Chilling outweighs photoperiod in preventing precocious spring development. Glob. Chang. Biol. 20, 170–182. https://doi.org/10.1111/gcb.12360.

Li, C., Stevens, B., Marotzke, J., 2015. Eurasian winter cooling in the warming hiatus of 1998–2012. Geophys. Res. Lett. 42, 2015GL065327. https://doi.org/10.1002/2015GL065327.

Li, H., Wang, C., Zhang, L., Li, X., Zang, S., 2017. Satellite monitoring of boreal forest phenology and its climatic responses in Eurasia. Int. J. Remote Sens. 38, 5446–5463. https://doi.org/10.1080/01431161.2017.1339925.

Linderholm, H.W., 2006. Growing season changes in the last century. Agric. For. Meteorol. 137, 1–14. https://doi.org/10.1016/j.agrformet.2006.03.006.

Lund, R., Reeves, J., 2002. Detection of undocumented changepoints: a revision of the two-phase regression model. J. Clim. 15, 2547–2554. https://doi.org/10.1175/1520-0442(2002)015<2547:DOUCAR>2.0.CO;2.

McCullough, D.G., Werner, R.A., Neumann, D., 1998. Fire and insects in northern and boreal forest ecosystems of North America. Annu. Rev. Entomol. 43, 107–127. https://doi.org/10.1146/annurev.ento.43.1.107.

Meehl, G.A., Arblaster, J.M., Fasullo, J.T., Hu, A., Trenberth, K.E., 2011. Model-based evidence of deep-ocean heat uptake during surface-temperature hiatus periods. Nat. Clim. Chang. 1, 360–364. https://doi.org/10.1038/nclimate1229.

Melaas, E.K., Friedl, M.A., Richardson, A.D., 2016. Multiscale modeling of spring phenology across deciduous forests in the eastern United States. Glob. Chang. Biol. 22, 792–805. https://doi.org/10.1111/gcb.13122.

Menzel, A., Fabian, P., 1999. Growing season extended in Europe. Nature 397, 659. https://doi.org/10.1038/17709.

Myneni, R.B., Keeling, C.D., Tucker, C.J., Asrar, G., Nemani, R.R., 1997. Increased plant growth in the northern high latitudes from 1981 to 1991. Nature 386, 698–702. https://doi.org/10.1038/386698a0.

Park, H., Jeong, S.-J., Ho, C.-H., Kim, J., Brown, M.E., Schaepman, M.E., 2015. Nonlinear response of vegetation green-up to local temperature variations in temperate and boreal forests in the Northern Hemisphere. Remote Sens. Environ. 165, 100–108. https://doi.org/10.1016/j.rse.2015.04.030.

Peng, S., Piao, S., Ciais, P., Myneni, R.B., Chen, A., Chevallier, F., Dolman, A.J., Janssens,

I.A., Peñuelas, J., Zhang, G., Vicca, S., Wan, S., Wang, S., Zeng, H., 2013. Asymmetric effects of daytime and night-time warming on Northern Hemisphere vegetation. Nature 501, 88–92. https://doi.org/10.1038/nature12434.

Peñuelas, J., Rutishauser, T., Filella, I., 2009. Phenology feedbacks on climate change. Science 324, 887–888. https://doi.org/10.1126/science.1173004.

Piao, S., Fang, J., Zhou, L., Ciais, P., Zhu, B., 2006. Variations in satellite-derived phenology in China's temperate vegetation. Glob. Chang. Biol. 12, 672–685. https://doi.org/10.1111/j.1365-2486.2006.01123.x.

Piao, S., Friedlingstein, P., Ciais, P., Viovy, N., Demarty, J., 2007. Growing season extension and its impact on terrestrial carbon cycle in the Northern Hemisphere over the past 2 decades. Glob. Biogeochem. Cycles 21, GB3018. https://doi.org/10.1029/2006GB002888.

Piao, S., Cui, M., Chen, A., Wang, X., Ciais, P., Liu, J., Tang, Y., 2011. Altitude and temperature dependence of change in the spring vegetation green-up date from 1982 to 2006 in the Qinghai-Xizang Plateau. Agric. For. Meteorol. 151, 1599–1608. https://doi.org/10.1016/j.agrformet.2011.06.016.

Pielke Sr., R.A., Avissar, R., Raupach, M., Dolman, A.J., Zeng, X., Denning, A.S., 1998. Interactions between the atmosphere and terrestrial ecosystems: influence on weather and climate. Glob. Chang. Biol. 4, 461–475. https://doi.org/10.1046/j.1365-2486.1998.t01-1-00176.x.

Pinzon, J.E., Tucker, C.J., 2014. A non-stationary 1981–2012 AVHRR NDVI3g time series. Remote Sens. 6, 6929–6960. https://doi.org/10.3390/rs6086929.

Richardson, A.D., Braswell, B.H., Hollinger, D.Y., Jenkins, J.P., Ollinger, S.V., 2009. Near-surface remote sensing of spatial and temporal variation in canopy phenology. Ecol. Appl. 19, 1417–1428. https://doi.org/10.1890/08-2022.1.

Richardson, A.D., Keenan, T.F., Migliavacca, M., Ryu, Y., Sonnentag, O., Toomey, M., 2013. Climate change, phenology, and phenological control of vegetation feedbacks to the climate system. Agric. For. Meteorol. 169, 156–173. https://doi.org/10.1016/j.agrformet.2012.09.012.

Rossi, S., Isabel, N., 2017. Bud break responds more strongly to daytime than night-time temperature under asymmetric experimental warming. Glob. Chang. Biol. 23, 446–454. https://doi.org/10.1111/gcb.13360.

Schoennagel, T., Balch, J.K., Brenkert-Smith, H., Dennison, P.E., Harvey, B.J., Krawchuk, M.A., Mietkiewicz, N., Morgan, P., Moritz, M.A., Rasker, R., Turner, M.G., Whitlock, C., 2017. Adapt to more wildfire in western North American forests as climate changes. PNAS 114, 4582–4590. https://doi.org/10.1073/pnas.1617464114.

Wang, X., Piao, S., Xu, X., Ciais, P., MacBean, N., Myneni, R.B., Li, L., 2015. Has the advancing onset of spring vegetation green-up slowed down or changed abruptly over the last three decades? Glob. Ecol. Biogeogr. 24, 621–631. https://doi.org/10.1111/geb.12289.

Wang, K., Zhang, T., Zhang, X., Clow, G.D., Jafarov, E.E., Overeem, I., Romanovsky, V., Peng, X., Cao, B., 2017. Continuously amplified warming in the Alaskan Arctic: implications for estimating global warming hiatus. Geophys. Res. Lett. 44, 2017GL074232. https://doi.org/10.1002/2017GL074232.

Way, Danielle A., Montgomery, Rebecca A., 2014. Photoperiod constraints on tree phenology, performance and migration in a warming world. Plant Cell Environ. 38, 1725–1736. https://doi.org/10.1111/pce.12431.

White, M.A., Hoffman, F., Hargrove, W.W., Nemani, R.R., 2005. A global framework for monitoring phenological responses to climate change. Geophys. Res. Lett. 32, L04705. https://doi.org/10.1029/2004GL021961.

Yu, H., Luedeling, E., Xu, J., 2010. Winter and spring warming result in delayed spring phenology on the Tibetan Plateau. PNAS 107, 22151–22156. https://doi.org/10.1073/pnas.1012490107.

Zeng, H., Jia, G., Epstein, H., 2011. Recent changes in phenology over the northern high latitudes detected from multi-satellite data. Environ. Res. Lett. 6, 045508. https://doi.org/10.1088/1748-9326/6/4/045508.

Zhang, X., Friedl, M.A., Schaaf, C.B., Strahler, A.H., Hodges, J.C.F., Gao, F., Reed, B.C., Huete, A., 2003. Monitoring vegetation phenology using MODIS. Remote Sens. Environ. 84, 471–475. https://doi.org/10.1016/S0034-4257(02)00135-9.